American Mineralogist, Volume 84, pages 1033–1040, 1999

^{23}Na, ^{29}Si, and ^{71}Ga MAS-NMR spectroscopy of synthetic gallian-fluor-amphiboles

BARBARA L. SHERRIFF,[1,*] DAVID M. JENKINS,[2] GERALD KUNATH-FANDREI,[3] STEFFEN GOETZ,[3] AND CHRISTIAN JÄGER[3]

[1]Department of Geological Sciences, University of Manitoba, Winnipeg, Manitoba R3T 2N2, Canada
[2]Department of Geological Sciences and Environmental Studies, Binghamton University, Binghamton, New York 13902-6000, U.S.A.
[3]Institüt für Optik and Quantenelectronik, Friedrich-Schiller-Universität, Max-Wien Platz 1, D-07743 Jena, Germany

ABSTRACT

A magic-angle-spinning nuclear magnetic resonance (MAS NMR) spectroscopic study was done on the series of synthetic gallian-fluor amphiboles to identify the extent of Ga and Si ordering in the tetrahedral sites. Assignment of the peaks in the complex ^{29}Si MAS NMR spectra of pargasitic amphiboles is based on observations of the gradual change in peak intensity and position as well as by comparison with computer simulations of the relative intensities of the ^{29}Si MAS NMR spectra for the amphiboles along the compositional join. The ^{29}Si spectra agree best with models that allow Ga on both the T1 and T2 sites, which supports the previous cation distribution results obtained by Rietveld refinement of powder X-ray diffraction data. It was not possible, however, to discriminate between cation distribution models that allowed completely random mixing of Ga and Si vs. the presence of Ga-O-Ga avoidance on the tetrahedral sites. Comparison of the very high speed ^{71}Ga MAS NMR spectra (35 kHz) with the distribution of Ga in octahedral and tetrahedral sites shows that the ratio of tetrahedral to octahedral site occupancy is vastly overestimated from the NMR spectra due to the large quadrupolar effects of the asymmetrical octahedral site. The ^{23}Na MAS NMR spectra of tremolite and Ga-substituted pargasites show a shift to higher frequency and increasing peak width with Ga content that can be related to the reduction in magnetic shielding produced by the substitution of Ga for Si and Mg.

INTRODUCTION

The compositional variations that are observed in natural calcic amphiboles are modeled, to a first approximation, by the join tremolite [$Ca_2Mg_5Si_8O_{22}(OH)_2$]-pargasite ($NaCa_2[Mg_4Al][Al_2Si_6]O_{22}(OH)_2$). These two end-members are related by the substitution of Na, $^{[6]}$Al, and $^{[4]}$Al into tremolite by the pargasite exchange, which is a 1:1 combination of the Al-tschermaks exchange $^{[6]}Al + {}^{[4]}Al = {}^{[6]}Mg + {}^{[4]}Si$ and the edenite exchange $Na + {}^{[4]}Al = \square + {}^{[4]}Si$ where $\square$ is a vacancy in the A site. Recent studies (Raudsepp et al. 1987; Welch et al. 1994, 1998; Jenkins and Hawthorne 1995; Oberti et al. 1995a, 1995b) have focused on determining the extent of cation order-disorder of the tetrahedrally and octahedrally coordinated cations in pargasitic amphiboles because this information is necessary to verify proposed mixing-on-sites activity-composition relationships (e.g., Sharma 1996) and to quantify configurational entropy from cation disorder. Magic-angle-spinning nuclear magnetic resonance (MAS NMR) spectroscopy, infrared (IR) spectroscopy, and X-ray Rietveld structure refinement on several chemical analogues of pargasite by Raudsepp et al. (1987) and the MAS NMR and IR spectroscopy of synthetic pargasite by Welch et al. (1994) helped to deduce the state of cation order-disorder. Raudsepp et al. (1987) concluded that octahedrally coordinated trivalent cations were significantly disordered with Mg over the M1, M2, and M3 sites in OH-bearing pargasites but relatively ordered at the M2 site in F-bearing pargasites. Various ^{29}Si NMR MAS spectra of scandian-fluor pargasite ($NaCa_2[Mg_4Sc][Al_2Si_6]O_{22}(OH)_2$) were compatible with substantial Si and Al disorder over the tetrahedrally coordinated sites, but the authors cautioned that their interpretation was not conclusive owing to the complex spectrum overlap and the unknown effect of octahedral-cation variation on the spectrum. Welch et al. (1994) concluded that there was disorder of Al and Mg over the M2 and M3 sites but that Al occurred only on the T1 tetrahedral site. Of particular interest here is the observation by Welch et al. (1994) that the ^{27}Al MAS NMR peak ratios gave a much higher $^{[4]}$Al/$^{[6]}$Al ratio than expected from the ideal chemistry (supported by electron microprobe analysis) of the synthetic pargasite they studied. Welch et al. (1994) suggested that quadrupolar effects for ^{27}Al may be responsible for the abnormally low intensity of the $^{[6]}$Al signal. By comparing the ^{29}Si spectra of various synthetic calcic and sodic-calcic amphiboles, Welch et al. (1998) concluded that Na in the A site of amphibole induces a shift in the T1(Si_3) [=Q^3(0Al)] by about 2.5 ppm to higher frequency compared to an amphibole with a vacant A site (e.g., tremolite), and that at least some long-range Al-Si disorder exists in pargasite as shown by the presence of a broad peak at –89 ppm, which the authors attributed to the presence of T1(Si_3) sites. Such sites would not be present in pargasite if all of the Al were ordered

*E-mail: bl_sherriff@umanitoba.ca

at the T1 tetrahedral site. Although the ^{29}Si spectrum of pargasite was simulated nicely by five peaks, Welch et al. (1998) preferred to interpret the spectrum on the basis of six peaks, suggesting that there was an overlap of two peaks at –82 ppm. Clearly the interpretation of the MAS NMR spectrum of pargasitic amphibole remains a complex issue.

This study presents the ^{29}Si, ^{71}Ga, and ^{23}Na MAS NMR spectra of a series of amphiboles along the gallian-fluor analogue of the tremolite-pargasite join, $Ca_2Mg_5Si_8O_{22}F_2$-$NaCa_2[Mg_4Ga][Ga_2Si_6]O_{22}F_2$. Cation-site occupancy information was reported by Jenkins and Hawthorne (1995) using Rietveld structure refinements of powder X-ray diffraction. The incorporation of Ga into the structure, though not identical to Al, has much better X-ray scattering power than Al and allows Ga to be located by X-ray diffraction techniques with fairly high precision. The use of fluorine was necessitated by the instability of the hydroxyl equivalent of this join. By examining this same series with the MAS-NMR technique, we can address several key issues: (1) how reliable are the existing tetrahedrally coordinated cation peak assignments for the ^{29}Si and ^{71}Ga spectra for amphiboles; (2) how do the individual ^{29}Si peak intensities vary with increasing and known Ga content on the T1 and T2 tetrahedral sites and, more importantly, how do they correspond with the predictions from simple cation-dispersion models; (3) how closely do the intensities of the ^{71}Ga spectra correspond to the known proportions of Ga in octahedral and tetrahedral coordination, and (4) what effect, if any, does the changing chemical environment in amphibole have on the ^{23}Na MAS NMR spectrum which, in turn, allows one to assess the sensitivity of the ^{23}Na spectrum to changes in its chemical vs. structural environment?

EXPERIMENTAL TECHNIQUES

Sample description

Samples were synthesized from mixtures of reagent-grade oxides and carbonates at 1000 °C and 3 kbar. The resultant amphiboles were relatively blocky and very fine grained (about 5×10 μm). Details of the synthesis and characterization are given by Jenkins and Hawthorne (1995). The site occupancies of Ga were determined from Rietveld structure refinements with a high degree of precision because of the strong X-ray scattering power of Ga relative to the other cations. The results indicated that octahedrally coordinated Ga was essentially ordered entirely on the M2 site. The tetrahedrally coordinated Ga was strongly partitioned onto the T1 site but with a small and relatively constant proportion (~20%) of the $^{[4]}$Ga occurring at the T2 site. Both the Rietveld refinements and electron microprobe analyses indicated that there was a slight excess of tetrahedral Ga, compared to octahedral Ga, over that expected from strict adherence to the pargasite exchange. Table 1 summarizes some key information about the samples.

Nuclear magnetic resonance spectroscopy

Various ^{29}Si and ^{23}Na MAS NMR spectra were obtained using a Doty MAS probe with a Bruker AMX-500 multinuclear Fourier transform spectrometer at the Prairie Regional NMR Centre in Winnipeg. Powdered samples of the amphiboles were spun at speeds of between 4 and 6 kHz at an angle of 54.7° to the magnetic field. These ^{29}Si MAS NMR spectra were recorded at a frequency of 99.3 MHz with 8192 data points, a spectral width of 50 kHz, 30° pulses. Trial spectra were obtained with delays between transients of between 5 and 300 s. There was no variation in relative peak height with changes in delay and as a 30s delay produced the best signal strength to experimental time ratio this was used to collect the spectra which were analyzed. These ^{23}Na MAS NMR spectra were obtained at a frequency of 132.3 MHz with 8192 data points, a spectral width of 125 kHz, 1 μs pulse length, and 0.3 s delay between pulses. Between 2000 and 9000 transients were recorded dependant upon the concentration of Na in the amphibole.

Various^{71}Ga MAS NMR spectra were obtained at the Institüt für Optik and Quantenelektronik, Friedrich-Schiller-Universität at a frequency of 121.98 MHz, a $\pi/8$ pulse length of 1 μs, spectral width of 625 kHz, using a Bruker 2.5 mm probe head with the sample spinning at a frequency of 28 kHz. This high spinning speed is necessary to reduce the large anisotropies of ^{71}Ga. Earlier attempts to obtain these spectra with a rotation speed of 14 kHz resulted in spinning sidebands from the tetrahedral peak overlapping the octahedral peak position. 17 168 transients were recorded for PARG 6-4 with a delay between pulses of 1 s and 343 765 for PARG 7-1 with a delay of 0.2s. A trial experiment with an empty rotor showed that there was no significant background intensity for ^{71}Ga. Peak positions were measured with reference to tetramethylsilane (TMS) for ^{29}Si, NaCl in aqueous solution for ^{23}Na and an aqueous solution of gallium chloride for ^{71}Ga.

Relative intensities of ^{29}Si peaks were inferred by simulating the spectra on a computer using a least-squares iterative process, which varied the isotropic chemical shift, the Gaussian and Lorentzian broadening parameters and the intensity of each line. The spectra of TREM 19-3 and PARG 10-1 had distinct spinning sidebands that were also simulated and their intensi-

TABLE 1. Nominal composition, synthesis products, selected cation site occupancies, and total Ga contents of the synthetic amphiboles

Sample	Nominal composition	Products*	Cation populations (apfu)†						ΣGa	
			T1-Si	T1-Ga	T2-Si	T2-Ga	M2-Mg	M2-Ga	Rietveld	EMP‡
TREM 19-3	$Ca_2Mg_5Si_8O_{22}F_2$	Amph, [Q]	4.0	0.0	4.0	0.0	2.0	0.0	0.0	0.0
PARG 10-1	$Na_{0.2}Mg_{4.8}Ga_{0.6}Si_{7.6}O_{22}F_2$	Amph, [Q,Sr1]	3.55(5)	0.45(5)	3.93(5)	0.07(5)	1.83(2)	0.17(2)	0.69(7)	0.66(9)
PARG 9-1	$Na_{0.4}Ca_2Mg_{4.6}Ga_{1.2}Si_{7.2}O_{22}F_2$	Amph, [Q,Sr1]	3.23(6)	0.77(6)	3.80(6)	0.20(6)	1.68(3)	0.32(3)	1.29(8)	1.18(5)
PARG 8-2	$Na_{0.6}Ca_2Mg_{4.4}Ga_{1.8}Si_{6.8}O_{22}F_2$	Amph, [Sr1,Q,Di]	2.94(6)	1.06(6)	3.83(7)	0.17(3)	1.58(3)	0.42(3)	1.6(1)	1.7(1)
PARG 7-1	$Na_{0.8}Ca_2Mg_{4.2}Ga_{2.4}Si_{6.4}O_{22}F_2$	Amph, [Sr1,Di]	2.67(6)	1.33(6)	3.59(8)	0.41(8)	1.36(3)	0.64(3)	2.4(1)	2.1(2)
PARG 6-4	$NaCa_2Mg_4Ga_3Si_6O_{22}F_2$	Amph,Sr2, [Di, Sp]	2.70(9)	1.30(9)	3.58(9)	0.42(9)	1.36(5)	0.74(5)	2.5(1)	2.43(9)

Notes: Data from Jenkins and Hawthorne (1995). Uncertainty in last digit shown in parentheses.
*Phase abbreviations: Amph = amphibole; Di = diopside; Q = quartz; Sr1 and Sr2 = gallian sapphirine 1 and 2; Sp = gallian spinel; [] = phase present at levels <5 wt%, otherwise phases are listed in order of decreasing abundance.
†Cation populations determined from powder X-ray diffraction Rietveld structural refinements.
‡Electron Microprobe data for amphibole crystals.

ties included in the calculation of relative intensities for each peak. Simulations of the spectra of PARG 8-2, PARG 9-1, PARG 10-1, and TREM 19-3 required broad peaks of between 60 and 130 kHz to account for raised baselines probably due to amorphous or poorly crystalline material. These broad peaks were not included in the calculations of relative intensity.

RESULTS

^{29}Si MAS NMR spectra

As expected, the Ga-free sample (TREM 19-3) has only two peaks in its spectrum, one at –92.4 and the other at –87.8 ppm, (Fig. 1a) that have been previously assigned to Si in the T1(Si_3) and T2(Si_2) sites, respectively (Smith et al. 1983). Even though there are equal numbers of T1 and T2 sites in the amphibole structure, the relative peak intensities of the center bands of the simulated spectrum are not identical, with the –92.4 ppm peak being slightly less intense (49.5% total peak intensity) and broader than the –87.8 ppm peak (50.5% total peak intensity) (Fig. 2a). Because this inequality of peak widths is not observed for OH-bearing amphiboles (Jenkins et al. 1997), the difference in peak width may be caused by dipolar or spin-spin coupling to adjacent magnetic ^{19}F nuclei, even though Si is not directly bonded to the anion in the O3 site (OH^- or F^-). The Si-O3 interatomic distance is shorter for the T1 site (3.48 Å) than for the T2 site (3.55 Å) according to the single-crystal refinement of fluor-tremolite by Cameron and Gibbs (1973), and thus the coupling constant would be slightly larger for T1 than T2. The difference in relative intensities increases from 1 to 8% when the spinning sidebands are included in the calculation (Table 2). This could be due to the accuracy of simulating these small peaks or to the difference in chemical shift anisotropies and dipolar couplings between the two sites. The difference between the calculated and measured values of relative intensity for this ordered structure allow an estimation of ±4% for the error in the calculation of relative intensities.

With the addition of Ga, these two peaks both decrease in relative intensity and broadening. As the amount of Ga in the amphibole increases other peaks appear (Figs. 1b–f). The peaks fitted to these envelopes of resonances by simulating the spectra are interpreted as being due to Si in T1(Si_2Ga) at about –84 ppm, T2(SiGa) at –80 ppm and T2(Ga_2) at –76 ppm (Fig. 2 b–f). In assigning the peaks, it was calculated (see below) that there would be too low a probability of there being Si in the T1(Ga_3) and T1(Ga_2Si) environments to produce measurable peak intensity. Therefore, peaks were not assigned to these atomic environments.

The production of new peaks at a higher frequency is consistent with the observed shift to higher frequency when Ga substitutes for Si in glasses (Sherriff and Fleet 1990) and in albite (Sherriff et al. 1991a) similar to the effect of the substitution of Si by Al. From Sherriff et al. (1991b), this shift to higher frequency is commensurate with an increase in the mean T-O distances, particularly the <T1-O> distance (Jenkins and Hawthorne 1995) and with the decreased bond valence of Ga when compared to Si. Sherriff and Fleet (1990) found that the amount of shift depends strongly on T-O-T bond angle varying from 4.2 ppm at 130° to 7.4 ppm at 170°. Here, the T1-O7-T1 and T1-O5-T2 angles decrease gradually by 10° from the Si to

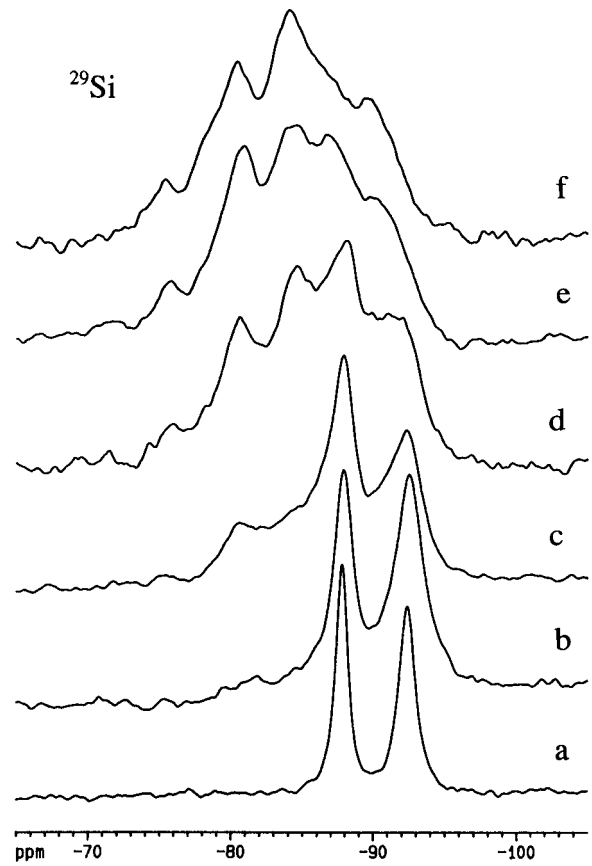

FIGURE 1. ^{29}Si MAS NMR spectra of $^{[4]}$Si in **(a)** TREM 19-3, **(b)** PARG 10-1, **(c)** PARG 9-1, **(d)** PARG 8-2, **(e)** PARG 7-1, and **(f)** PARG 6-4.

TABLE 2. Relative intensities and chemical shifts (ppm) of observed ^{29}Si MAS NMR peaks

Sample	Si (apfu)*	T2(Ga_2)	T2(SiGa)	T1(Si_2Ga)	T2(Si_2)	T1(Si_3)
TREM 19-3†	7.96	–	–	–	54% (–87.8)	46% (–92.4)
PARG 10-1†	7.48	–	9% (–81.5)	–	48% (–87.9)	43% (–92.5)
PARG 9-1	7.08	–	14% (–80.8)	17% (–84.6)	35% (–87.6)	34% (–92.1)
PARG 8-2	6.76	0.4% (–76.3)	18% (–80.5)	27% (–84.4)	37% (–87.8)	16% (–91.8)
PARG 7-1	6.56	4% (–76.0)	20% (–80.4)	26% (–84.2)	22% (–86.3)	29% (–90.8)
PARG 6-4	6.45	8% (–75.0)	19% (–79.5)	54% broad (–84.5)‡		20% (–89.8)

Notes: Relative intensity calculated as percentage of amphibole peaks. Chemical shift (ppm) in parentheses.
*From EMPA.
†Relative intensities of both spinning sidebands and center bands are included in the total relative intensities.
‡Sum of both Ti (Si_2Ga) and T2 (Si_2).

the Ga end-members. As the XRD data gives an average of Si and Ga containing sites, it is probable that the increase in angle is underestimated for O atoms adjacent to Ga.

The incorporation of Ga into the octahedral sites in place of Mg and of Na into the A-site also causes changes in the magnetic shielding at the tetrahedral sites and hence in ^{29}Si chemical shift similar to the effect found by Millard and Luth (1998) in Di-CaTs clinopyroxenes. In a study of the scapolite mineral series, Sherriff et al. (1987) showed that the substitution of Na by Ca in adjacent octahedral sites gave a shift of about 1 ppm. As the narrowest peak observed in these spectra (–92.4 ppm peak of TREM 19-3) has a peak width at half maximum of 1.5 ppm (150Hz), the variation in adjacent octahedral cations would cause broadening and distortion of the peaks due to overlapping peaks that cannot be individually resolved. This effect is clearly shown in the asymmetrically broad T1(Si_3) peak at –92.4 ppm in the

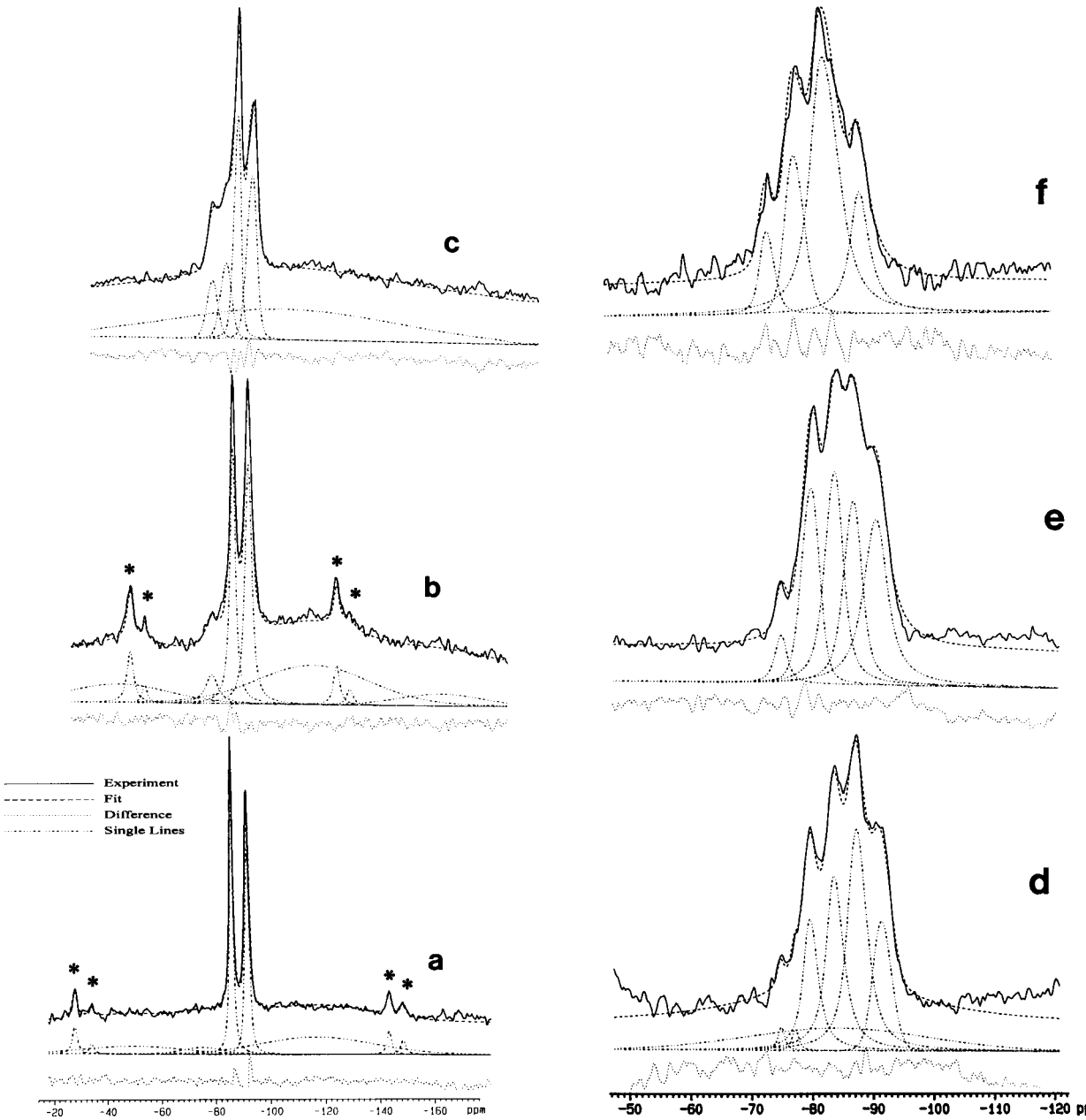

FIGURE 2. Simulations of ^{29}Si MAS NMR spectra for **(a)** TREM 19-3, **(b)** PARG 10-1, **(c)** PARG 9-1, **(d)** PARG 8-2, **(e)** PARG 7-1, and **(f)** PARG 6-4. Spinning sidebands are marked with asterisks.

spectrum of PARG 9-1 (Fig. 1c) as compared with the symmetrical narrow peak at –92.4 in the spectrum of TREM 19-3 and PARG 10-1 (Figs. 1a and 1b, respectively).

^{71}Ga MAS NMR Spectra

Allocation of the peaks in the ^{71}Ga spectra (Fig. 3) to Ga environments was made taking into consideration the 5.7 times greater chemical shift range of ^{71}Ga than ^{27}Al for solutions (Akitt 1987). Bradley et al. (1993) found a linear relationship between ^{71}Ga and ^{27}Al isotropic chemical shifts in tetrahedral and octahedral sites in solids. Using the equation of Bradley et al. (1993) and the ^{27}Al spectrum of pargasite from Welch et al. (1994), one would predict a single ^{71}Ga tetrahedral peak to be at about 190 ppm and two ^{71}Ga octahedral peaks to be at –20 and +20 ppm. Massiot et al. (1995) reports, from static NMR, the isotropic chemical shift of the tetrahedral site of **b**-Ga_2O_3 to be at 200 ppm. In view of these earlier studies, we attribute the prominent peak at 230 ppm to tetrahedrally coordinated Ga. There is a quadrupolar doublet in the spectra of PARG 6-4 that is attributed to octahedrally coordinated Ga at about 40 ppm. However, it is possible that even these low intensity peaks are from the gallian sapphirine contamination in this sample, as discussed below.

^{23}Na MAS NMR spectra

These ^{23}Na MAS NMR spectra are all very similar with one broad peak at about –23 ppm (not shown). There is a slight shift in peak position with increasing Ga substitution into neighboring tetrahedral sites from –23 ppm for PARG 10-1 to –27 ppm for PARG 6-4 as well as an increase of about 400 Hz in peak width. This is similar to the effect on individual ^{29}Si peaks of replacing adjacent Si or Mg with Ga.

Mineral impurities

The mineral impurities in the amphibole consist of quartz, diopside, and two gallian-sapphirines of varying Mg and Ca contents (Table 1). In the ^{29}Si MAS NMR spectra of TREM 19-3, PARG 10-1, PARG 9-1, and PARG 8-2 the baselines are raised between –100 and –125 ppm, which were fitted with very broad peaks (Figs. 2a–d). This may be due to amorphous Si that would be invisible by XRD or to instrumental artifacts. These broad peaks were not included in the calculations of relative intensities of the Ga-amphibole peaks even though they have relatively high intensity. The exclusion of these broad peaks from the calculations may increase the error in the relative intensities of individual peaks

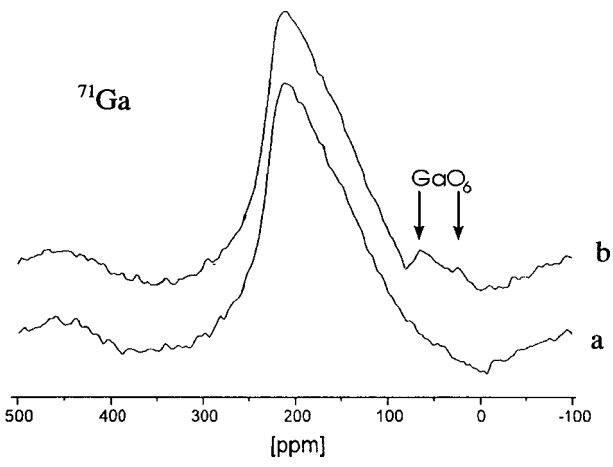

FIGURE 3. ^{71}Ga MAS NMR spectra of $^{[6]}$Ga and $^{[4]}$Ga in the most Ga-rich samples. **(a)** PARG 7-1. **(b)** PARG 6-4.

Although quartz is found by XRD in all samples except PARG 7-1 and 6-4, there is no signal due to quartz at –107.1 ppm in the ^{29}Si NMR spectra. This could be because quartz, especially pure synthetic samples, tends to have a very long relaxation time and can be invisible even when it constitutes up to 30% of the sample (Sherriff and Hartman 1985). Diopside, which is present in samples PARG 8-2, PARG 7-1, and PARG 6-4, has a ^{29}Si isotropic chemical shift of –84.8 ppm (Sherriff et al. 1991b). In these samples there is a small bump on the side of the large –84 ppm peak but as this is no larger than the background noise it was not considered to be worth simulating these peaks. However this would cause an overestimation in the relative intensity of the –84 ppm peak for PARG 8-2, PARG 7-1, and PARG 6-4. Therefore the –84 ppm peak was not used in the comparison of observed and modeled spectra.

The Ga-sapphirine phases in PARG 9-1, 8-2, and 7-1 have a composition $Mg_{3.75}Ca_{0.60}Ga_{7.05}Si_{2.60}O_{20}$ whereas those in PARG 6-4 are more Ca rich with a composition of $Mg_{2.85}Ca_{1.55}Ga_{7.30}Si_{2.30}O_{20}$ (Jenkins and Hawthorne 1995). To investigate the result of this contamination by sapphirine, ^{29}Si MAS NMR spectra were obtained from samples of synthetic Mg rich ($Mg_3CaGa_8Si_2O_{20}$ = GASA 5-1) and Ca rich ($Mg_2Ca_2Ga_8Si_2O_{20}$ = GASA 2-2) Ga-sapphirine (Figs. 4a and 4b, respectively). Our spectrum of Mg-rich Ga sapphirine has peaks at –71.8, –74.8, –76.2, and –77.4 ppm in ratios of approximately 4:2:1:1 (Fig. 4a). The shape of these spectra is very similar to those obtained by Christy et al. (1992) on a series of Mg-Al-sapphirine samples, which had peaks at –73.1, –75.5, –78.0, and –80.0 ppm. These peaks were assigned to $Q^3(Al_3)$, $Q^3(Al_2Si)$, $Q^3(AlSi_2)$, and $Q^3(Si_3)$ respectively. The difference of 1–2 ppm between values for Ga-Mg-sapphirine and Al-Mg sapphirine can be explained by the replacement of Al by Ga (Sherriff and Fleet 1990). The spectrum of Ca rich Ga-sapphirine is very different (Fig. 4b) with two peaks of equal intensity at –74.8 and –78.0 ppm. In this study we simply present the data for comparison with the amphibole spectra and do not interpret ordering in sapphirine. There are small peaks in the ^{29}Si MAS NMR spectra of PARG 9-1, 8-2, 7-1, and 6-4 that could be correlated with the peaks of Ga-sapphirine but most are not significantly higher than the background noise and therefore were not separately considered in the calculations of relative intensities of peaks.

DISCUSSION

^{29}Si MAS NMR spectra

The suite of amphibole compositions studied here should provide a crucial test of currently accepted assignments for the ^{29}Si spectra for pargasite and/or provide further insights into the variations of these peak intensities with changing cation content with known, long-range tetrahedral Si and Ga distribu-

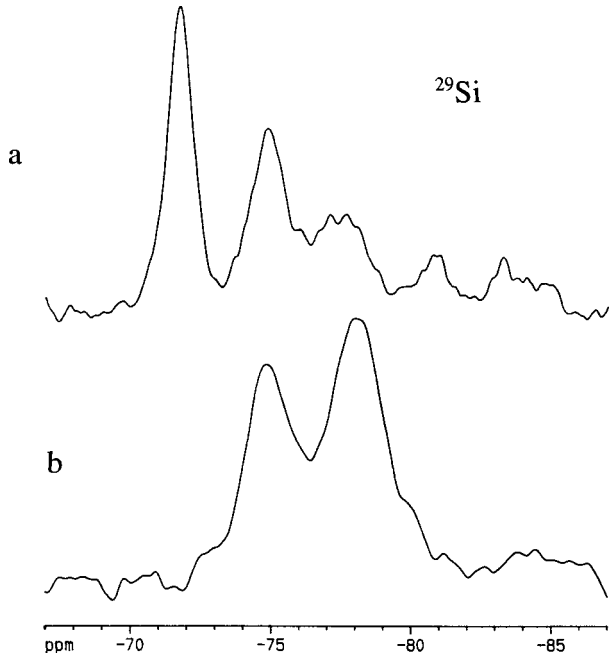

FIGURE 4. ^{29}Si MAS NMR spectra of Ga-sapphirine. **(a)** Mg-rich GASA 5-1. **(b)** Ca-rich GASA 2-2.

tions. To aid in predicting the number of next nearest neighbor (NNN) configurations about the four tetrahedral T1 and four T2 positions per formula unit cell of amphibole, a computer program was written (AMPHTET) that builds a one-dimensional amphibole chain by randomly dispersing Ga between the T1 and T2 sites according to (1) the cumulative (long-range) limits of Ga content on the T1 and T2 sites and (2) with or without the imposition of Ga-O-Ga avoidance, the Ga equivalent of Al-O-Al avoidance as is commonly imposed for tetrahedrally coordinated Al (Lowenstein 1954). The condition of local-balance or homogeneous-dispersion of charges, which is often applied to layered silicates (e.g., Herrero et al. 1985), was not explicitly built into the program. This condition can, however, be approximated by adjusting the probability sufficiently high that a particular site will be filled by Ga to ensure rapid "saturation" of the Ga content to the average value of the mineral but not so high that the Ga distribution within an individual six-member ring (segment of the double chain) becomes a fully ordered pattern.

In amphibole, Si residing in the T1 site is bonded to three NNN tetrahedral cations (2 T2 and 1 T1) which produces four possible NNN configurations for Si in a T1 site: Si surrounded by three Si (Si_3), by two Si and one Ga (Si_2Ga), by two Ga and one Si ($SiGa_2$), and by three Ga (Ga_3). Similarly, Si in a T2 site is bonded to only two other tetrahedral (T1) cations, giving only three possibilities: Si surrounded by two Si (Si_2), by one Si and one Ga (SiGa), by two Ga (Ga_2). Table 3 shows the relative proportions of NNN configurations that are predicted for the cases of the presence of Ga-O-Ga avoidance (model 1), a random distribution of Ga and Si, both of which must adhere to the average Ga contents of the T1 and T2 sites for the whole crystal (model 2), and the case where Ga only occurs on the T1 site and obeys Ga-O-Ga avoidance (model 3). The AMPHTET program, when run with the condition of Ga-O-Ga avoidance, produces T2(Si_2) and T2(SiGa) relative abundances that are in exact agreement with those predicted from the theoretical treatment of Welch et al. (1998).

The differences between the observed and calculated relative intensities for each peak of each sample for each of the tree above models are shown in Figure 5. The mean difference is 4.4% for model 1, 4.1% for model 2, and 5.5% for model 3. Thus, no significant difference exists between models 1 and 2 but model 3 is slightly less feasible. Therefore the observed peak areas of the ^{29}Si MAS NMR spectra agree best with models based on Ga distributed over both the T1 and T2 sites but do not allow us to say unambiguously whether Ga-O-Ga avoidance occurs or not. The overall agreement between the predicted and observed ^{29}Si MAS NMR peak areas lends support to the peak assignments.

Examination of the ^{29}Si MAS NMR spectra in Figure 1 and the associated assignments of NNN atomic configurations in Table 2 illustrates the effect that a change in the bulk mineral composition has on the spectra. In going from fluor-tremolite to gallian-fluor-pargasite, there is a noticeable shift to higher frequency for the T1(Si_3) peak, from –92.4 to –89.8 ppm. This

TABLE 3. Proportions of Si NNN configurations averaged over 80,000 sites as predicted under several limiting conditions

Sample	Ga on T2 (apfu)	Ga on T1 (apfu)	T2 (relative%)			T1 (relative%)			
			Ga_2	SiGa	Si_2	Ga_3	$SiGa_2$	Si_2Ga	Si_3
TREM 19-3 (same for all conditions)	0	0	0	0	50	0	0	0	50
PARG 10-1 Avoidance	0.07	0.45	0	12	41	0	0.2	7	40
PARG 10-1 No avoidance	0.07	0.45	0	12	41	0	0.2	7	40
PARG 10-1 All Ga on T1	–	0.52	0	14	40	0	0	7	40
PARG 9-1 Avoidance	0.20	0.77	0.7	20	33	0	2	13	31
PARG 9-1 No avoidance	0.20	0.77	0.4	20	33	0	1	13	32
PARG 9-1 All Ga on T1	–	0.97	2.0	22	32	0	0	14	29
PARG 8-2 Avoidance	0.17	1.06	3.6	24	29	0	2	16	25
PARG 8-2 No avoidance	0.17	1.06	2	25	29	0	1	15	27
PARG 8-2 All Ga on T1	–	1.23	6	25	28	0	0	18	23
PARG 7-1 Avoidance	0.41	1.33	10	22	25	0	7	20	16
PARG 7-1 No avoidance	0.41	1.33	7	24	27	0	4	20	20
PARG 7-1 All Ga on T1	–	1.74	12	31	21	0	0	28	8
PARG 6-4 Avoidance	0.42	1.30	9	24	24	0	7	20	16
PARG 6-4 No avoidance	0.42	1.30	6	24	27	0	4	19	20
PARG 6-4 All Ga on T1	–	1.72	12	30	21	0	0	27	9

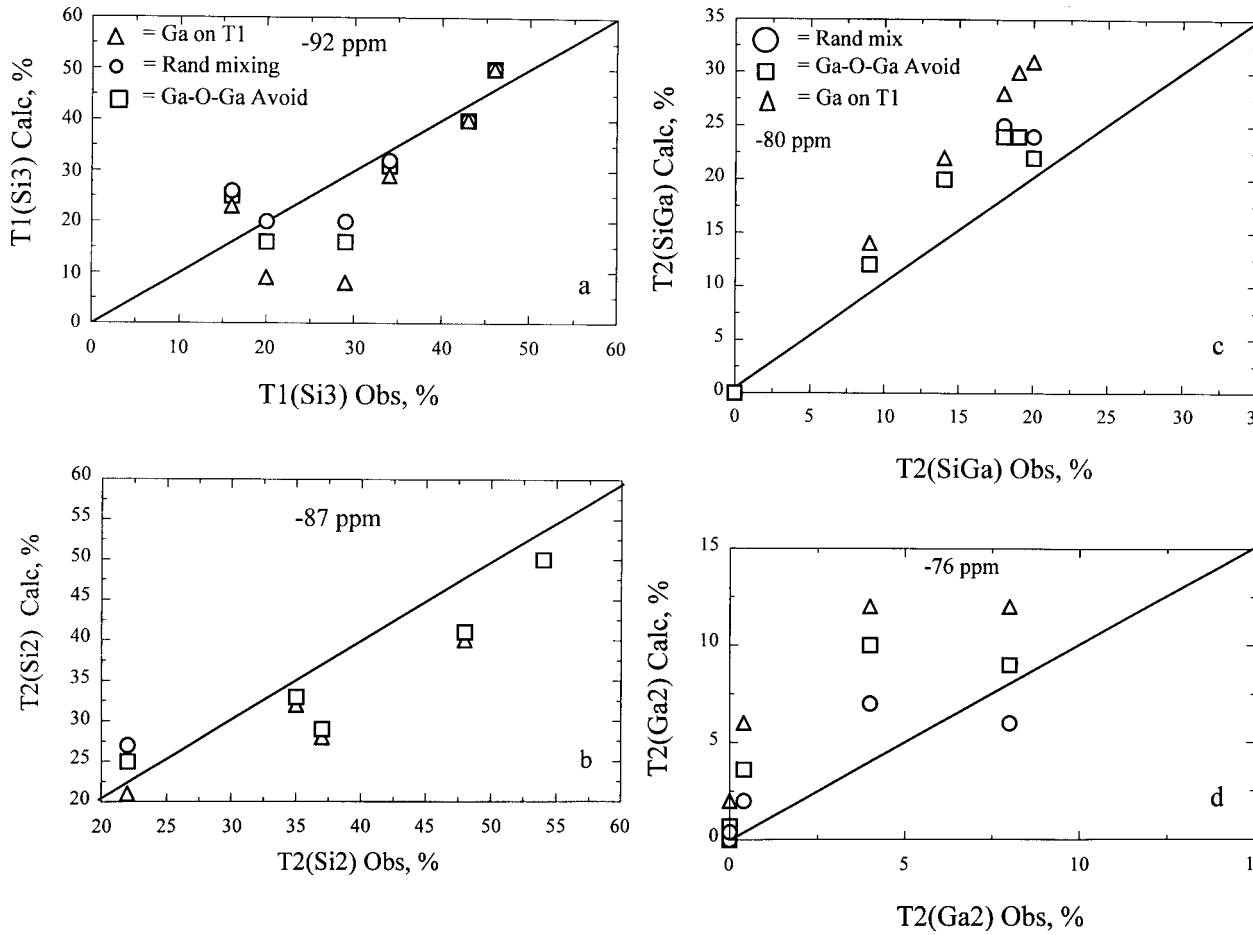

FIGURE 5. Comparison of calculated and observed relative 29Si MAS NMR peak intensities for the peaks at **(a)** –92 ppm, **(b)** –87 ppm, **(c)** –80 ppm, and **(d)** –76 ppm. Symbols: squares = Model 1, Ga-O-Ga avoidance; circles = Model 2, random mixing; filled triangles = Model 3, all Ga in T1 site. The straight lines represent 1:1 correlations.

magnitude of chemical shift is commensurate with the gradual filling of the A site by Na, as observed by Welch et al. (1998). Indeed, there is, in general, very close agreement in ^{29}Si peak assignments for the most pargasitic amphiboles studied here (PARG 7-1, 6-4) and the fluor-edenite and pargasite studied by Welch et al. (1998), with both studies assigning the –89 ppm peak to T1(Si_3), the –86 ppm peak to T2(Si_2), and the –84.5 ppm peak to T1(Si_2Ga/Al). In both this study and that of Welch et al. (1998) the highest frequency peaks are assigned to the T2 site configurations with no or only 1 Ga (Al) cation NNN; however, the positions of these peaks are noticeably different, with the T2(Ga_2) and the T2(SiGa) being –75 and –80 ppm, respectively, in this study, and being –79 and –82 ppm, respectively, in Welch et al. (1998). This difference is attributed to the substitution of Ga for Al in the present study and not just to the presence of Na in the A site, which is present in both gallian-fluor-pargasite and pargasite.

^{71}Ga MAS NMR spectra

Comparison of the observed and predicted octahedral and tetrahedral ^{71}Ga peak intensities could shed some light on the interpretation of the ^{27}Al spectra, which has proven problematic for certain common silicates. For example, Circone et al. (1991) noted the pronounced excess of tetrahedral relative to octahedral Al for their phlogopite-eastonite series and could not readily explain it. Similarly, Welch et al. (1994) in their study of synthetic pargasite also observed more tetrahedral than octahedral Al based on the ratios of NMR peaks. In both of these cases the authors did not have independent (i.e., X-ray diffraction) information on the distribution of octahedral and tetrahedral Al, aside from the bulk chemistry of the samples. Such a mis-match between observed and predicted partitioning of octahedral vs. tetrahedral Al was not observed for chlorite (Welch et al. 1995).

With the Ga-F-pargasites, we do have independent information on the octahedral and tetrahedral Ga contents and observe that the tetrahedral to octahedral ratios from the NMR spectra do not correspond to those from the XRD data. The ratio of the tetrahedral to octahedral site occupancy by Ga from the Rietveld refinement is 2.3:1 for PARG 6-4 and 2.7:1 for PARG 7-1. Therefore the intensity of the octahedral peak in both ^{71}Ga spectra should be about one-third of the tetrahedral

peak. Even the small quadrupolar doublet observed in the ^{71}Ga spectrum of PARG 6-4 may be due to contamination by Ga-sapphirine. The lack of octahedral peak intensity is likely to be due to the larger asymmetry and therefore quadrupolar moment of this site with respect to the tetrahedral site. Massiot et al. (1995) were unable to obtain an MAS peak from the octahedral site of -Ga_2O_3 due to the large quadrupolar moment despite there being equal proportions of octahedral and tetrahedral Ga present. They obtained the isotropic chemical shift and quadrupolar parameters using a combination of static and spin echo techniques. The loss of signal due to quadrupolar effects may be greater for ^{71}Ga than for ^{27}Al due to the quadrupolar width factor for ^{71}Ga being 2.34 times that for ^{27}Al. Akitt (1987) observes that even in solution the width factor appears to be greater than calculated for ^{71}Ga.

APPLICATIONS

There are two main insights obtained from this study which are of direct application to our understanding of the crystal chemistry of amphiboles and of Al-bearing minerals in general. First, there is very good agreement between the predicted and observed peak intensities for the ^{29}Si MAS NMR spectra when Ga is allowed to reside on both the T1 and T2 octahedral sites. Such cation disorder on the tetrahedral sites is not only in agreement with the previous XRD Rietveld structure refinements of Jenkins and Hawthorne (1995) but lends further support to the growing opinion that there can be much more disorder of trivalent cations over the tetrahedral sites of amphibole than customarily believed. At issue is the temperature dependency of this cation disorder, which, to date, has only been observed in natural amphiboles equilibrated at high temperatures (Oberti et al. 1995a) or in synthetic amphiboles made at temperatures of 900–1000 °C (Welch et al. 1998; this study). Knowledge of the temperature and bulk-composition dependence of Al-Si cation disorder in pargasitic amphiboles would help immensely in deducing the thermal history of natural hornblende-bearing assemblages. Second, using the relative peak areas of the MAS NMR spectra of quadrupolar nuclei (e.g., ^{27}Al, ^{71}Ga) for deducing the relative proportions of tetrahedral vs. octahedral trivalent cations without accounting for the quadrupolar broadening effects, may lead to a significant under-estimation of the amount of octahedral cations present in the structure. This may account, in part, for the abnormally high $^{[4]}$Al/$^{[6]}$Al ratios observed in the study of phlogopitic micas by Circone et al. (1991) and pargasite by Welch et al. (1994). In this study, the $^{[6]}$Ga MAS NMR signal is only observable in the most Ga-rich sample (PARG 6-4) despite its presence in all but the fluor-tremolite sample. Even then the $^{[6]}$Ga MAS NMR signal may, unfortunately, be attributable to other $^{[6]}$Ga-rich phases present.

ACKNOWLEDGMENTS

This research was funded by an NSERC operating grant and University Research Fellowship Award to B.L.S. and NSF grant EAR-9628212 to D.M.J. Thanks to J. Brewster, University of Manitoba, for help with the statistical interpretation of the data and to Mark Welch and an anonymous reviewer for comments on this manuscript.

REFERENCES CITED

Akitt, J.W. (1987) Aluminium, Gallium, Indium and Thallium. In J. Mason, Ed., Multinuclear NMR, chapter 9. Plenum Press, New York.

Bradley, S.M., Howe, R.F., and Kydd, R.A. (1993) Correlation between ^{27}Al and ^{71}Ga NMR chemical shifts. Magnetic Resonance in Chemistry, 31, 883–886.

Cameron, M. and Gibbs, G.V. (1973) The crystal structure and bonding of fluor-tremolite: A comparison with hydroxyl tremolite. American Mineralogist, 58, 879–888.

Christy, A.G., Phillips, B.L., Güttler, B.K., and Kirkpatrick, R.J. (1992) A ^{27}Al and ^{29}Si MAS NMR and infrared spectroscopic study of Al-Si ordering in natural and synthetic sapphirines. American Mineralogist, 77, 8–18.

Circone, S., Navrotsky, A., Kirkpatrick, R.J., and Graham, C.M. (1991) Substitution of $^{[6,4]}$Al in phlogopite: Mica characterization, unit-cell variation, ^{27}Al and ^{29}Si MAS-NMR spectroscopy, and Al-Si distribution in the tetrahedral sheet. American Mineralogist, 76, 1485–1501.

Herrero, C.P., Sanz, J., and Serratosa, J.M. (1985) Si, Al distribution in micas: analysis by high-resolution ^{29}Si NMR spectroscopy. Journal of Physics C: Solid State Physics, 18, 13–22.

Jenkins, D.M. and Hawthorne, F.C. (1995) Synthesis and Rietveld refinement of amphibole along the join $Ca_2Mg_5Si_8O_{22}F_2$-$NaCa_2Mg_4Ga_3Si_6O_{22}F_2$. Canadian Mineralogist, 33, 13–24.

Jenkins, D.M., Sherriff, B.L., Cramer, J., and Xu, Z. (1997) Al, Si, and Mg occupancies in tetrahedrally and octahedrally coordinated sites in synthetic aluminous tremolites. American Mineralogist, 82, 280–290.

Lowenstein, W. (1954) The distribution of aluminum in the tetrahedra of silicates and aluminates. American Mineralogist, 39, 92–96.

Massiot, D., Farnan, I., Gautier, N., Trumeau, D., Trokiner, A., and Coutoures, J.P. (1995) ^{71}Ga and ^{69}Ga nuclear magnetic resonance study of β-Ga_2O_3: resolution of four and six coordinated Ga sites in static conditions. Solid State Nuclear Magnetic Resonance, 4, 241–248.

Millard, R.L. and Luth, R.W. (1998) Tetrahedral Si/Al distribution in DiCaTs clinopyroxenes using 29Si MAS NMR. EOS Transactions of the American Geophysical Union, 79, S162 (M21B6).

Oberti, R., Ungaretti, L., Cannillo, E., Hawthorne, F.C., and Memmi, I. (1995a) Temperature-dependent Al order-disorder in the tetrahedral double-chains of *C2/m* amphiboles. European Journal of Mineralogy, 7, 1049–1063.

Oberti, R., Hawthorne, F.C., Ungaretti, L., and Cannillo, E. (1995b) $^{[6]}$Al disorder in amphiboles from mantle peridotites. Canadian Mineralogist, 33, 867–878.

Oberti, R., Sardone, N., Hawthorne, F.C., Raudsepp, M., and Turnock, A.C. (1995c) Synthesis and crystal-structure refinement of synthetic fluor-pargasite. Canadian Mineralogist, 33, 25–31.

Raudsepp, M., Turnock, A.C., Hawthorne, F.C., Sherriff, B.L., and Hartman, J.S. (1987) Characterization of synthetic pargasitic amphiboles ($NaCa_2Mg_4M^{3+}Si_6Al_2O_{22}(OH,F)_2$; M^{3+}=Al, Cr, Ga, Sc, In) by infrared spectroscopy, Rietveld structure refinement and ^{27}Al, ^{29}Si and ^{19}F MAS nmr spectroscopy. American Mineralogist, 72, 580–593.

Sharma, A. (1996) Experimentally derived thermochemical data for pargasite and reinvestigation of its stability with quartz in the system Na_2O-CaO-MgO-Al_2O_3-SiO_2-H_2O. Contributions to Mineralogy and Petrology, 125, 263–275.

Sherriff, B.L. and Fleet, M.E. (1990) Local ordering in gallium- and germanium-substituted glasses investigated by MAS NMR. Journal of Geophysical Research, 95, B10, 15727–15732.

Sherriff, B.L. and Hartman, J.S. (1985) High resolution ^{29}Si NMR of feldspars: Si/Al disorder and the effects of paramagnetics. Canadian Mineralogist, 23, 203–212.

Sherriff, B.L., Grundy, H.D., and Hartman, J.S. (1987) Occupancy of T sites in the scapolite series. A multinuclear NMR study using magic angle spinning. Canadian Mineralogist, 25, 717–730.

Sherriff, B.L., Fleet, M.E., and Burns, P.C. (1991a) Tetrahedral site ordering in synthetic gallium albite: A ^{29}Si MAS NMR study. Journal of Solid State Chemistry, 94, 52–58.

Sherriff, B.L., Grundy, H.D., and Hartman, J.S. (1991b) The relationship between ^{29}Si MAS NMR chemical shift and silicate mineral structure. European Journal of Mineralogy, 3, 751–768.

Smith, K.A., Kirkpatrick, R.J., Oldfield, E., and Henderson, D.M. (1983) High-resolution silicon-29 nuclear magnetic resonance spectroscopic study of rock forming silicates. American Mineralogist, 68, 1206–1215.

Welch, M.D., Kolodziejski, W., and Klinowski, J. (1994) A multinuclear NMR study of synthetic pargasite. American Mineralogist, 79, 261–268.

Welch, M.D., Barras, J., and Klinowski, J. (1995) A multinuclear NMR study of clinochlore. American Mineralogist, 80, 441–447.

Welch, M.D., Liu, S., and Klinowski, J. (1998) ^{29}Si MAS NMR systematics of calcic and sodic-calcic amphiboles. American Mineralogist 83, 85–96.

MANUSCRIPT RECEIVED SEPTEMBER 9, 1998
MANUSCRIPT ACCEPTED FEBRUARY 7, 1999
PAPER HANDLED BY JONATHAN F. STEBBINS